DR JIANBING YAN (Orcid ID : 0000-0001-8650-7811)

Article type : Original Article

An allele of *ZmPORB2* encoding a protochlorophyllide oxidoreductase promotes tocopherol accumulation in both leaves and kernels of maize

Wei Zhan[1], Jie Liu[1], Qingchun Pan[1], Hong Wang[1,2], Shijuan Yan[3], Kun Li[1], Min Deng[1,4], Wenqiang Li[1], Nannan Liu[1], Qian Kong[3], Alisdair R. Fernie[5], Jianbing Yan[1*]

[1]National Key Laboratory of Crop Genetic Improvement, Huazhong Agricultural University, Wuhan, 430070, China

[2] College of Agronomy, Hebei Agricultural University, Hebei Sub-center of National Maize Improvement Center of China, Key Laboratory of Crop Germplasm Resources of Northern China (Ministry of Education), Baoding, 071001, China

[3]Agro-biological Gene Research Center, Guangdong Academy of Agricultural Sciences, Guangzhou, 510640, China

[4] College of Agronomy, Hunan Agricultural University, Changsha, 410128, China

[5] Max Planck Institute of Molecular Plant Physiology, 14476 Potsdam-Golm, Germany

[*] Address correspondence to: Jianbing Yan (yjianbing@mail.hzau.edu.cn)
Phone: +86-27-87280110 FAX: 86-27-87280016

Running title: ZmPORB2 promotes tocopherol accumulation in maize

Keywords: Tocopherol, QTL-mapping, Phytol, Maize (*Zea mays*), *ZmPORB2*.

Summary

Phytol is one of the key precursors for tocopherol synthesis in plants, however, the underlying mechanisms concerning the accumulation of tocopherol remain poorly understood. In this study, *qVE5*, a major QTL affecting tocopherol accumulation in maize kernels was identified via a positional cloning approach. *qVE5* encodes a protochlorophyllide oxidoreductase (*ZmPORB2*), which localizes to the chloroplast. Overexpression of *ZmPORB2* increased tocopherol content in both leaves and kernels. Candidate gene association analysis identified a 5/8-bp insertion/deletion (InDel058) in the 5'UTR as the causal polymorphism in affecting *ZmPORB2* expression and being highly associated with tocopherol content. We showed that higher expression of *ZmPORB2* correlated with more chlorophyll metabolites in the leaf following pollination. RNA-sequencing and metabolic analysis in near isogenic lines (NILs) support that *ZmPORB2* participates in chlorophyll metabolism enabling the production of phytol--an important precursor of tocopherol. We also found that the tocopherol content in the kernel is mainly determined by the maternal genotype, a fact that was further confirmed by *in-vitro* culture experiments. Finally, a PCR-based marker based on Indel058 was developed in order to facilitate the high tocopherol (vitamin E) maize breeding.

Introduction

Vitamin E was discovered in 1922 and was subsequently characterized as an important antioxidant. It plays an important role in the maintenance of cardiovascular health, alleviation of cancer development, maintenance of immune system functioning as well as neuro- and skin- protection in humans (Wolf, 2005; Azzi, 2007; Clarke *et al.,* 2008; Galli and Azzi, 2010; Frank *et al.,* 2012). Despite the relatively low incidence of acute vitamin E deficiency, many adults who have suboptimal tocopherol levels cannot achieve optimal health (Péter *et al.,* 2016). Vitamin E is an essential micronutrient of human diets. Unfortunately, daily diets often fail to provide adequate vitamin E in both developing and developed countries (Jiang *et al.,* 2005; Ford *et al.,* 2006). Therefore, vitamin E biofortification in staple crops would provide an ideal means by which to relieve vitamin E deficiency (Fitzpatrick *et al.,* 2012).

The vitamin E family is comprised of tocopherols and tocotrienols and each contains four isoforms respectively, all of which can only be synthesized in photosynthetic organisms (Horvath *et al.,* 2006; Maeda & DellaPenna, 2007; Mene-Saffrane & DellaPenna, 2010). In

plants, tocopherol content is elevated in response to a variety of abiotic and biotic stresses (Collakova & DellaPenna, 2003a; Ledford *et al.*, 2004). It also accumulates in seeds to prevent lipid peroxidation during seed storage, germination, and early seedling development (Sattler *et al.*, 2004).

The tocopherol biosynthesis pathway has been well studied in *Arabidopsis thaliana* and *Synechocystis* sp. PCC6803 by transgenic and mutagenesis studies (DellaPenna, 2005; DellaPenna & Mène-Saffrané, 2011). The committed step is the homogentisate phytyltransferase (HPT)-catalysed condensation of homogentisate (HGA) and phytol-diphosphate (PDP) to produce 2-methyl-6-phytyl-1, 4-benzoquinol (MPBQ). This reaction is classically considered to be the rate-limiting step, controlling the production of the immediate precursor to the tocopherol pathway (Collakova & DellaPenna, 2003b). Increasing the size of the PDP pool is, thus likely, an efficient way to improve tocopherol biosynthesis. A recent study showed that the PDP supply for tocopherol synthesis depends on the release of phytol from chlorophyll (Vom Drop *et al.*, 2015). Phytol phosphorylation is proceeded in two steps--with the chemical reactions being catalyzed by phytol kinase (*VTE5*) and phytol-phosphate kinase (*VTE6*), respectively, in order to produce PDP (Valentin *et al*., 2006; Vom Dorp *et al.*, 2015). Free phytol can be either derived from a salvage pathway or from chlorophyll breakdown (Ischebeck *et al.*, 2006; Hörtensteiner & Krautler, 2011). During senescence, chlorophyll breakdown in photosynthetic tissue is visible since leaves lose their green color whilst color also changes during the maturation of the kernel and ripening of fruit. Chlorophyllides (Chlide), pheophorbide (Pheide), pheophytin and phytol are the major products of chlorophyll breakdown via the PHEOPHORBIDE A OXYGENASE (PAO) pathway, (Hörtensteiner & Krautler, 2011; Hörtensteiner, 2013). Pheophytin pheophorbide hydrolase (PPH) specifically hydrolyzes pheophytin, which releases a large amount of phytol (Schelbert *et al.*, 2009; Hörtensteiner, 2013). Chlorophyll turnover also occurs during the photosystem repair in response to biotic and abiotic stresses. However, the chlorophyll content remains steady during this cycle (Matile *et al.*, 1999; Beisel *et al.*, 2010). This chlorophyll-salvage cycle also releases phytol. Recently, chlorophyllase (CLH1, CLH2) and PPH were found to be dispensable for tocopherol accumulation in seed during chlorophyll breakdown (Zhang *et al.*, 2014). However, chlorophyll synthase (CHLG) may affect chlorophyll and tocopherol synthesis in *Arabidopsis* (Zhang *et al.*, 2015). Recent studies suggested that chlorophyll dephytylase1 (CLD1) has chlorophyll de-phytylation activity which can, in combination with CHLG, form a salvage cycle of chlorophyll turnover (Lin *et*

al., 2014; Lin *et al.,* 2016) (Figure 1). Nevertheless, the contribution of chlorophyll breakdown and turnover to tocopherol biosynthesis-related phytol production remains to be fully clarified.

Linkage mapping and association studies are now commonly used to dissect the biochemistry and genetic basis of maize quantitative traits (Xiao *et al.,* 2017). Progresses regarding tocopherol synthesis in maize kernel revealed that a few major, and several minor QTLs contribute to vitamin E content and a few QTLs are co-localized with core tocopherol genes (Wong *et al.,* 2003; Chander *et al.,* 2008; Xu *et al.,* 2012). *ZmVTE4* (γ-tocopherol methyltransferase) has been identified through genome-wide and candidate gene association analysis and two markers within *ZmVTE4* were developed (Li *et al.,* 2012; Lipka *et al.,* 2013). Recently, many QTLs were identified by using large-scale QTL mapping and a number of candidate genes were identified, including several genes involved in and outside the known tocopherol biosynthetic pathways (Diepenbrock *et al.,* 2017; Wang *et al.,* 2018). In this study, a major QTL (*qVE5*) affecting tocopherol content in the maize kernel was identified by linkage analysis in three bi-parental mapping populations. Positional cloning of *qVE5* revealed that the protochlorophyllide oxidoreductase encoding gene *ZmPORB2* underlies *qVE5*, which is supported with transgenic experiments. Further experiments revealed that tocopherol accumulation in leaf sharply increased after pollination, and that tocopherol synthesis in maize kernel is promoted by *ZmPORB2* presumably with support from the leaf. Finally, we posit that a PCR marker derived from the causative polymorphism of ZmPORB2 could be utilized in high vitamin E maize breeding.

Results

Fine mapping of a major QTL for vitamin E, *qVE5*

Three RIL populations, including F_{10} RILs generated by crossing Zong3 and Yu8701 (ZY) and then selfing, F_6 RILs from the hybrid of K22/CI7 (KC), and F_9 RILs whose parental lines are B73and BY804 (BB), containing 170-188 lines (Pan *et al*., 2016), were genotyped with high-density SNPs and phenotyped in two environments, respectively. A major QTL, *qVE5*, for γ-tocopherol and total tocopherol content in kernel was mapped to chromosome 5 in all three populations in multiple environments (Table S1; Figure S1; Wang *et al.,* 2018). *qVE5* accounted for a large proportion of phenotypic variation in each RIL population ranging from 9.75% in BB to 42.47% in KC population for γ-tocopherol content (Table S1). In the KC population, *qVE5* explained the largest proportion of the phenotypic variation (Table S1) and

was narrowed down to a 3.46-Mb interval (Figure 2a). To identify *qVE5*, a heterogeneous inbred family (HIF-1171) in the 3.46-Mb region was selected from the F_6 generation of the cross K22/CI7 (Liu *et al.*, 2016). HIF-1171 was heterozygous in a region flanked by markers PZA03161.1 (13.58Mb) and PZA02058.1 (29.27Mb), covering a 15.69Mb genomic region harboring *qVE5* (Figure 2b). A total of 11 HIF-1171 plants were self-pollinated to produce 11 F_2 populations. Clear co-segregation was observed in the 12SY1171-2 families, indicating that the *qVE5* is in this region (Figure S2). Nine recombinants in the 4-Mb target region were then identified from 1620 individuals by using two markers--NF129 and NF11. The progenies of the nine recombinants were planted in Sanya in 2013, in Beijing and Sanya in 2014. *qVE5* was then narrowed down to the region between NF781 and SNP96, which covered a 170-kb genomic interval in the B73 reference genome (V2) (Figure 2c). For the K22 genome, the interval is located on a single bacterial artificial chromosome (BAC) clone covering approximately 157.9kb region. Only one predicted gene, GRMZM2G073351, encoding a protochlorophyllide oxidoreductase (*ZmPORB2*, *Zmpor2*) was identified in the target region in both the B73 and the K22 genome (Figure 2d). Therefore, *ZmPORB2* was chosen as the candidate gene of *qVE5*.

Overexpression of *ZmPORB2* increased tocopherol content in leaves and kernels

To demonstrate the function of *ZmPORB2* in the determination of tocopherol content in maize kernel, a 4.3-kb genomic fragment covering *ZmPORB2* genomic coding sequence was amplified from B73 with p351-F/R (Table S2) and its expression in maize was driven by 35S promoter. The verified clone was transformed into maize inbred line C01 by *Agrobacterium tumefaciens*-mediated transformation. Three independent transgenic T_0 plants (*PORB*#1, *PORB*#4, and *PORB*#6) were selected to produce T_1 families. Quantitative real-time PCR (qPCR) showed 5- to 8-fold change in *ZmPORB2* mRNA abundance in leaves of transgenic plants at the six-leaf stage over that in control plants (empty vector) (Figure S3a). Moreover, the total tocopherol content was increased significantly by 28.11% to 50.59% at the six-leaf stage (Figure S3b). The percentage increase of tocopherol levels in transgenic maize kernels was smaller, compared with that in leaves, ranging from 18.12% to 19.24% more than that of the controls (Figure S3c). Overexpression experiments thus further confirmed that *ZmPORB2* is the causative gene of *qVE5* and its expressionincreases tocopherol content in both leaf and kernel in maize.

ZmPORB2 is localized in chloroplast and shows a high similarity to *PORB*

Protochlorophyllide reductases (*PORs*) are highly conserved in higher plants (Figure 3a). In *Arabidopsis*, three *PORs* were identified and named as *PORA*, *PORB*, and *PORC* (Frick *et al*., 2003). In maize, there is one *PORA* and two *PORB* homologs, denoted as *ZmPORA* (GRMZM2G084958), *ZmPORB1* (GRMZM2G036455) and *ZmPORB2* (GRMZM2G073351). To determine the subcellular localization of ZmPORB2, the full-length coding sequence of *ZmPORB2* was fused to GFP in the transient expression vector 35S::-GFP. After infiltration into maize leaf protoplasts, 35S::ZmPORB2-GFP fusion proteins exclusively co-localized with autofluorescence signals of the chloroplast, as observed for the PORBs in other higher plants (Reinbothe *et al.*, 1995; Masuda *et al.*, 2003; Sakuraba *et al.*, 2013), indicating that the ZmPORB2 protein is localized in the chloroplast (Figure S4).

To confirm whether the expression of *ZmPORBs* is associated with light conditions like its orthologs in other higher plants (Reinbothe *et al*., 1995; Masuda *et al.*, 2003; Sakuraba *et al.*, 2013; Heyes *et al.*, 2005; Scrutton *et al.*, 2012), the expression of the *ZmPORBs* was examined at ten time points within a 24-hour interval in a leaf from plants at the five-leaf stage under a normal diel light regime. The expression of *ZmPORB1* in the seedling was very low but was slightly elevated by light exposure in both short-day and long-day condition. Compared with *ZmPORB1*, *ZmPORB2* was expressed at a much higher level and was significantly induced by light exposure, reaching peak expression at 9h during long-day light exposure (Figure 3b). Furthermore, *ZmPORs* in maize have significantly different expression patterns at different developmental stages and following pollination, *ZmPORB2* shows the highest expression in leaves (Figure S5ab).

InDel058 likely affects kernel tocopherol content by altering *ZmPORB2* expression

ZmPORB2 contains four exons and encodes a protein of 396 amino acid residues. 18 SNPs and nine Indels were detected among the six parental alleles within the coding region. The eight SNPs in exons were synonymous, which excluded the possibility that the variation of tocopherol content in the RILs was caused by ZmPORB2 protein function. A number of large structural variations were identified by comparing the K22 with B73 (CI7-like) sequence (Figure 2d), including a 23,585-bp insertion located only 377 bp upstream of *ZmPORB2* transcription starting site in K22 genome. To investigate whether the 23,585-bp InDel affects the phenotype, primers (Table S2) were developed to amplify this large insertion in a diverse

association mapping panel (AMP508, Yang *et al.*, 2011). Surprisingly, the 23,585-bp InDel showed neither significant association with the *ZmPORB2* mRNA expression level nor with the total tocopherol content in the kernel (Figure S6ab).

To determine the causal mutation(s) in *ZmPORB2* that is responsible for the variation of expression levels and tocopherol content, the full-length genomic DNA of the *ZmPORB2* gene, including its 363-bp upstream and 106-bp downstream region, was re-sequenced in AMP508. In total, 45 variants (11 InDels and 34 SNPs) with minimum frequency >0.05 were identified and used for candidate gene association mapping. Indel058 was the site showing the strongest association with the γ-tocopherol (*P*=3.67E-13, Figure 4a) and total tocopherol content (*P*=1.81E-13, Figure 4a). Indel058 was located 59 bp upstream of ATG within the 5' untranslated region (UTR, Figure 4b). Indel058 and the other significant SNPs or InDels were located within a strong linkage disequilibrium (LD) block (Figure 4c).

Indel058 classified AMP508 into three prevalent haplotypes: allele0 (260 lines) with no insertion, allele5 (76 lines) with a 5-bp insertion, allele8 (168 lines) with an 8-bp insertion and other types (four lines). Indel058 is the only variation segregating in all three RIL populations, suggesting that it might be the causal polymorphism. Parents with high tocopherol content (BY804, CI7 and Zong3) carried allele0, parents with low tocopherol content carried allele5 (B73) or allele8 (K22 and YU8701) (Figure 4d). No significant differences were detected between groups with allele5 and allele8 in either γ- or total tocopherol content in the kernel or the *ZmPORB2* expression in kernel as evidenced in previously published RNA-seq data (Fu *et al.*, 2013). However, the allele0 group has significantly higher expression level of *ZmPORB2* (*P*=9.65E-15) than the group with insertion (allele5 and allele8) with increased γ-tocopherol (*P*=1.26E-12) and total tocopherol content (*P*=3.57E-11) (Figure 4e).

Dramatic change in tocopherol content and *ZmPORB2* expression in flag leaves after pollination

The expression of *ZmPORB2* was mainly detected in flag leaves and embryo but was negligible in the endosperm across the experimental time periods (Figure S5ab). After pollination, *ZmPORB2* expression becomes predominant among the three PORs in leaf (Figure S5ab). In order to determine whether the change of *ZmPORB2* expression is pollination dependent or just developmental stage related, near isogenic lines (14SY-NIL-2-8-5, Figure2c) with differences in the *ZmPORB2* allele (NIL^{K22}, NIL^{CI7}) were used and half of

NIL^{K22} and NIL^{CI7} plants were self-pollinated, while the rest were non-pollinated by bagging the ears throughout flowering time for expression analysis. The flag-leaves from the pollinated plants (P-Leaf) and from the non-pollinated plants (NP-Leaf) were collected for RNA extraction and tocopherol measurement (γ-, α-, and total tocopherol) on 0, 4, 6, 8, 10, 12, 16, and 20 days after pollination (DAP; except 0 DAP for NP-Leaf), respectively. For expression analysis, total RNA of the embryo and the endosperm was extracted from self-pollinated kernels collected at corresponding time points (10 DAP to 20 DAP, four time points).

The expression in the embryo exhibited fluctuations and a clear differences was observed between NIL^{CI7} and NIL^{K22} at 10 DAP (*P*=0.0142) to 16 DAP (*P*=5.28E-03) (Figure 5a, top panel). The expression level in the NP-Leaf remains low from 4 DAP to 16 DAP until a peak expression at 20 DAP, with no significant differences between the NILs (Figure 5a, middle panel). The expression of *ZmPORB2* in the P-Leaf reached a peak level on 8 DAP followed by a gradual decrease to the bottom at 16 DAP (Figure 5a, bottom panel). Higher expression levels in NIL^{CI7} were observed at the five different time points from 6 DAP (*P*=7.46E-03) to 16 DAP (*P*=3.81E-04) in the P-Leaf compared with those in NIL^{K22}. In the NP-Leaf γ-, α-, and total tocopherol contents remained stable at a low level, while in the P-Leaf, α- and total tocopherol contents started to increase at the beginning of pollination and reached the highest level at 16 DAP with a significantly higher level being attained in the NIL^{CI7} background (Figure 5c), consistent with the dynamics of *ZmPORB2* expression in this tissue (Figure 5a). Although significant changes were detected in the P-Leaf tocopherol content, its peak abundance was not reached until 16 DAP compared with the peak of *ZmPORB2* expression at 8 DAP. Interestingly, in the leaf, γ-tocopherol did not vary much and was maintained at a relatively low level (Figure 5bc) and α-tocopherol is the most abundant tocopherol component in the leaf and an approximate 5-fold increase was observed in pollinated over non-pollinated homozygous NILs at 16 DAP (Figure 5bc). However, in kernel, γ-tocopherol is the most abundant tocopherol component, with a significant difference between the two NILs (Figure S2). These data revealed that the gene function of *ZmPORB2* is affected largely by pollination thus affecting tocopherol accumulation in kernel.

ZmPORB2 participates in chlorophyll metabolism and tocopherol biosynthetic pathways

In plants, *PORB* is expressed in a light-dependent manner and encodes an enzyme that requires photons to catalyze the reduction of protochlorophyllide in the synthesis of

chlorophyll (Heyes *et al.,* 2005; Scrutton *et al.,* 2012). *PORB* is not directly involved in the tocopherol biosynthetic pathway (Figure 1). However, our results show that *ZmPORB2* significantly affects the tocopherol content in flag leaf. To position the *ZmPORB2* gene in the pathway, Pchlide(the substrate of *PORB*) levels, Chlide a (the product of *PORB*) levels, pheophorbide a levels, and phytol levels were measured in the flag-leaves of the NILs of both pollinated and non-pollinated plants.

From 0 DAP to 20 DAP, with the increase in *ZmPORB2* expression in the P-Leaves, chlorophyll (a+b) contents were stable and no differences were observed between those in the leaves of pollinated and non-pollinated NILs (Figure 6a). There was also no differences in Pchlide content between NIL^{K22} and NIL^{CI7} in either the P- or the NP-Leaves at 12 DAP (Figure 6b). A significant differences in Chlide a content was identified between NIL^{K22} and NIL^{CI7} at 12 DAP in both the P- and the NP-Leaves (Figure 6c). In the two homozygous *ZmPORB2* NILs, Pchlide and Chlide a content was significantly increased in the P-Leaves compared with the NP-Leaves at 12 DAP (Figure 6bc). By contrast, the content of Pheophorbide a in the P-Leaves remained unchanged at 12 DAP compared with NP-Leaves, and there was no differences in the levels of Pheophorbide a between NIL^{CI7} and NIL^{K22} (Figure 6d). Phytol content was, as expected, elevated in the P-Leaves compared with NP-Leaves at 12 DAP. Notably, a significant differences was observed between the levels of Phytol between NIL^{CI7} and NIL^{K22} in the P-Leaves (P=2.34E-04) but not in the NP-Leaves (P=0.2648) (Figure 6e).

We also examined the expression levels of some core genes involved in the vitamin E biosynthesis pathway (*VTE2*, *VTE4*, *VTE5*) and one important for chlorophyll synthesis (*CHLG*), which was reported to affect tocopherol synthesis in *Arabidopsis* (Zhang *et al*., 2015). *CHLG* expression started to rise when *ZmPORB2* expression sharply increased in the P-Leaves but not in the NP-Leaves. The *CHLG* expression pattern was very similar to that of *ZmPORB2* in the P-Leaves (Figure 6f). The expression levels of *VTE2* (Figure 6g), *VTE4* (Figure 6h), and *VTE5* (Figure 6i) also increased from 6 DAP and reached their highest levels at 10 or 16 DAP, and then decreased on 20 DAP. The increase in tocopherol synthesis and the expression of these genes in leaves showed similar trends. These data collectively indicate that *ZmPORB2* participates both in chlorophyll metabolism and tocopherol biosynthetic pathways in maize flag leaf.

Tocopherol accumulation in the kernel is highly associated with the maternal *ZmPORB2* genotype

Since both the expression of *ZmPORB2* and the tocopherol content changed drastically during seed development stages after pollination, we suspected that pollination might be one of causes for these changes. To address this question, in addition to the two self-pollinated homozygous kernels (NIL^{K22}, NIL^{CI7}), we also obtained the reciprocal hybrids between the NILs, including the hybrid kernels NIL^{K22CI7}-harvested from plants NIL^{K22} pollinated with the pollen of NIL^{CI7}, and NIL^{CI7K22}-- harvested from plants NIL^{CI7} plants pollinated with the pollen of NIL^{K22}. Mature hybrids and homozygous kernels were used to measure tocopherol content with γ-, α-, and total tocopherol being determined. Significant differences in kernel tocopherol content were observed between NIL^{CI7} and NIL^{K22} as well as between NIL^{K22CI7} and NIL^{CI7K22}. The maternal plants harboring the CI7 *ZmPORB2* allele had significantly higher γ-, α- and total tocopherol content in mature kernels (NIL^{CI7}, NIL^{CI7K22}) than those harboring the K22 *ZmPORB2* allele in mature kernels (NIL^{K22}, NIL^{K22C17}) (Figure 7). There were, however, no differences between the self-pollinated homozygous kernels of NIL^{CI7} and hybrid kernels of NIL^{CI7K22}. The same results were observed between kernels of NIL^{K22} and kernels of NIL^{K22C17} (Figure 7). However, in the progeny test based on the NIL family, the γ-tocopherol and total tocopherol content in the mature kernels of heterozygous maternal genotype was very close to the mid-parent value, demonstrating the additive effect of *ZmPORB2* (Figure S2). These results implied that tocopherol content in mature kernels related with ZmPORB2 function is largely dependent on the genotype of tissues other than the kernels.

The above conclusion is further supported by results from an *in vitro* kernel culture experiment in which kernels were excised from cob sections of two homozygous NILs of *ZmPORB2* at 18 DAP and cultured *in vitro* for five days with phytol (0% and 0.1%, v/v). No differences in embryo weight between the two lines were detected in all three growth conditions(Figure 8a). The kernels of both genotypes in plants from 18 DAP to 23 DAP exhibited obvious tocopherol accumulation, and the total tocopherol content in NIL^{CI7} was always significantly higher than that in NIL^{K22} (Figure 8b**).** The total tocopherol content in kernels cultured *in vitro* with supplementary phytol was significantly higher than that of kernels cultured without phytol. However, there was no differences in total tocopherol content in kernels between the two genotypes under either culture conditions. *ZmPORB2*

expression can be detected in the embryo at 18 DAP, with significant differences in *ZmPORB2* expression between the genotypes. However, *ZmPORB2* expression was barely detected among the culture conditions and 23 DAP (Figure 8c), indicating that the expression of *ZmPORB2* in kernels is accelerated by signals from tissues other than the kernel.

Discussion

ZmPORB2 is the gene underlying the tocopherol content QTL *qVE5*

In this study, we determined that *ZmPORB2* is the gene underlying the major QTL *qVE5* affecting tocopherol content in both leaf and kernel in maize. This finding was confirmed by expression and candidate gene association analyses as well as the generation and analysis of transgenic plants. *ZmPORB2* encodes a protochlorophyllide oxidoreductase which is conserved in higher plants. Time course analysis showed that *ZmPORB2* expression is light-dependent like that of the other PORB genes (Figure 3ab). The protein ZmPORB2 locates to the chloroplast (Figure S4), consistent with the chloroplast localization of the proteins encoded by other genes in the tocopherol biosynthesis pathway.

ZmPORB2 affects tocopherol synthesis in leaf after pollination

In the green tissues of higher plants, *PORA* expression is repressed and *PORB* becomes the most predominantly expressed *POR* gene. It is furthermore the only POR isoform catalyzing the light-driven reduction of protochlorophyllide (Pchlide) into chlorophyllide (Chlide) following the reproductive growth stage (Masuda *et al.,* 2003; Sakuraba *et al.,* 2013; Reinbothe *et al.,* 1995). Two *PORB* genes were identified in maize, but only *ZmPORB2* is highly expressed in the leaf after pollination--these findings imply that *ZmPORB2* rather than *ZmPORB1* predominantly executes *PORB* function in the leaf (Figure S5ab). The expression of *ZmPORB2* in the P-Leaf but not in the NP-Leaf started to increase at the beginning of pollination, reaching to a peak at 8 DAP. Meanwhile, a large amount of tocopherol (primarily α-tocopherol) was detected in flag leaves after pollination, being 10-20 times more abundant than that in the NP-Leaf. Significant differences in the tocopherol level and *ZmPORB2* expression were also observed between the leaves of two NILs from 0 DAP to 20 DAP (Figure 5c).

PORB is a chlorophyll biosynthesis associated gene that participates in chlorophyll metabolism in photosynthetic tissues such as the leaf. We have provided evidence that *ZmPORB2* executes PORB enzyme function since the levels of Chlide a--the product of PORB in plants--differ significantly between the NILs (Figure 6bc). However, no differences

were observed in the levels of chlorophyll (a+b) or pheophorbide a, which is a committed intermediate and metabolic marker for further chlorophyll breakdown via the pheophorbide a oxygenase (PAO) pathway (Hörtensteiner, 2013). As was shown using the Arabidopsis *vte6* mutant in a previous study, phytol derived from chlorophyll is the predominant precursor for tocopherol biosynthesis (Vom dorp *et al.,* 2016). Our finding implies that the phytol used for tocopherol production was unlikely provided by the conversion of pheophytin a to pheophorbide a catalyzed by pheophytinase (PPH). (Figure 6a, d). These results are consistent with previous findings in *Arabidopsis* (Zhang *et al.,* 2014) and more recently in maize (Diepenbrock *et al.,* 2017).

ZmPORB2 may play an essential role in balancing photosynthetic efficiency and oxidative damage. As the most abundant form of tocopherol in the chloroplast, α-tocopherol is an important antioxidant (Havaux *et al.,* 2005). Maize, like other plants, needs to constantly maintain photosynthetic efficiency. However, photosynthesis inevitably leads to oxidative damage of the photosystems, hence if not repaired, the activity of photosystem will decrease via a process termed "photoinhibition" (Tyystjärvi, 2013). Phytol may result from chlorophyll turnover, a cycle of chlorophyll synthesis and degradation. This cycle is related to photosystem repair and stability (Pokorska *et al.,* 2009; Hörtensteiner, 2013; Lin *et al.,* 2016). During this process, phytol is released but a substantial portion of the chlorophyllide and phytol yielded are recycled for the biosynthesis of new chlorophyll (Vavilin & Vermaas, 2007). The results of our study indicate that kernel tocopherol levels are strongly affected by steps outside the kernel. It is currently difficult to establish the form in which precursors for tocopherol biosynthesis is transported. Nevertheless, our data strongly support a role for the maternal tissues in the determination of kernel tocopherol levels. If phytol, or indeed any other lipophilic molecule is transported, the action of a yet unidentified lipid transfer protein is required. The exact mechanism of tocopherol intermediate transfer remains unresolved in the current study and will be difficult to untangle. That said spatial-temporal resolution following stable isotope labeling may represent a route by which this can be ascertained and existing mass-spectrometry-based technique can be carried out. The labelled substance could be phytol, or other metabolites related to chlorophyll pathways. Since metabolites transfer rapidly, finding the substrates and transporters for long distances between tissues is an important concern in the future.

ZmPORB2 affects tocopherol content in kernel probably by generating more precursors in leaf

In this study, the considerable expression of the tocopherol synthesis genes (*VTE 1-6*) in kernels (Support Data S1) and in the *in vitro* experiment in which phytol was supplied exogenously both confirm that tocopherol biosynthesis can occur within the developing kernel. However, tocopherol synthesis in non-photosynthesizing kernels is not independent of photosynthetic tissues, since phytol is a crucial precursor for tocopherol biosynthesis which is released majorly from chlorophyll and therefore chlorophyll is required to support large demands of phytol for tocopherol biosynthesis in kernels. *ZmPORB2* is a light-dependent enzyme which requires photons for the reduction of protochlorophyllide (Heyes *et al.,* 2005; Scrutton *et al.,* 2012, Gabruk & Mysliwa-Kurdziel, 2015). *ZmPORB2* was highly expressed in the leaf after pollination, and very weakly expressed in the embryo or kernel before 18 DAP, being expressed only at levels approximately 1/100 to 1/60 compared to those found in the leaf (Figure 5, Figure S5). These findings are similar with the recent study which assumed that the large amounts of phytol needed for tocopherol biosynthesis in maize embryos are from "a cycle involving repeated removal and efficient reesterification of phytol" (Diepenbrock *et al.,* 2017). In the present study, we found that tocopherol accumulation in kernels depends on the maternal--rather than the kernel-- genotypes by comparing the tocopherol contents in kernels between the reciprocal hybrids (Figure 7). An *in vitro* kernel culture experiment feeding phytol also proved that the precursors (i.e. phytol) for tocopherol biosynthesis in maize developing kernels could come from other tissues, independent of their *de novo* synthesis within kernels. According to these observations, we propose an alternative hypothesis that high expression of *ZmPORB2* in the leaf supports chlorophyll turnover following pollination providing precursors which can transfer to kernels for tocopherol synthesis.

ZmPORB2 is a target for high-nutrition maize breeding

Overexpression of *ZmPORB2* could elevate total tocopherol contents in maize leaf by up to 50% and in kernels by 19%, which renders it a good target for high vitamin E maize breeding. With the exception of *vte2*, which affects total tocopherol accumulation, several genes involved in the tocopherol biosynthesis pathway, such as *vte3* and *vte4*, only change the levels of individual tocopherol components without altering total tocopherol content (Shintani

& DellaPenna, 1998; Cheng *et al.*, 2003; Van Eenennaam *et al.*, 2003). Maize leaves can also accumulate high levels of tocopherols, especially α-tocopherol, which accumulate to much higher levels than in kernels. This presents an opportunity to improve the tocopherol content in silage maize for high-quality meat production. The natural variation of InDel058 located in the 5'UTR region affects the expression of *ZmPORB2* both in leaf and in kernel and thereby affects the tocopherol contents in different tissues. A PCR-based molecular marker (ID861) was developed (Table S2) and could be used for marker-assisted high vitamin E maize breeding. High expression of *ZmPORB2* could also be combined with *VTE4* (Li et al., 2012) to precisely tailor both the total tocopherol level and the accumulation of α-tocopherol which shows the highest vitamin E activity..

METHODS

The association panel, RIL populations and field trials.

The association mapping panel AMP508 was from a global maize collection, including temperate and tropical/subtropical elite inbred lines with detailed information documented in a previous study (Yang *et al.*, 2011). The AMP508 panel for tocopherol measurement was grown in three locations: Yunnan (Kunming), Chongqing, and Hainan (Sanya) of China in 2009, as described previously (Li *et al.*, 2012).

Six inbred lines were chosen from AMP508 to develop three recombinant inbred line (RIL) populations--namely B73/BY804 (BB), ZONG3/YU8701 (ZY), and K22/CI7 (KC)--for linkage analysis (Xiao *et al.*, 2016; Pan *et al.*, 2016). The 197 RILs from ZY and 175 RILs from KC, were planted in Yunnan (Kunming) and Chongqing in 2011. The 197 RILs from BB were planted in Yunnan (Kunming) and Hainan (Sanya) in 2011.

All the inbred lines, including the association panel and three RIL populations, were self-pollinated in each location.

QTL mapping and fine mapping

RIL populations were genotyped with Illumina MaizeSNP50 BeadChip and high-density genetic maps were constructed (Pan *et al.*, 2016). Composite interval mapping (CIM) implemented in WinQTLCart2.5 (Zeng *et al.*, 1999; Wang, 2012) was performed as detailed in the user manual. QTL detection was set at 0.5 cM scanning intervals between markers and a window size of 10 cM for tocopherol traits. The LOD threshold for QTL detection was set at > 3.0, and the confidence interval represented two-LOD drop from the peak.

HAZU-1171, a residual heterozygous segment line derived from the K22/CI7 RIL population (Liu et al., 2016), harbors a major QTL for kernel tocopherol content, named *qVE5* (Wang et al., 2018) which is flanked by markers NF129 and NF11 on chromosome 5. To fine map *qVE5*, HAZU-1171 was self-pollinated and 9 F_2 populations derived from the selected recombinants were planted in the winter of Sanya, China in 2012. A larger F_2 population, 12SY1171-2, with 62 individuals was used to validate this QTL by progeny test (Figure S2). The heterozygous plants were planted from the 2012 to 2014 to screen recombinants. Recombinants of more than ten haplotypes were selected for progeny tests. Finally, a pair of near isogenic lines (14SY-NIL-2-8-5) differ in ~170 kb for *qVE5* were utilised for further phenotypic evaluations.

Molecular marker development

Based on the B73 genome sequence (www.MaizeGDB.org) in the QTL region, SSR-based PCR markers were designed using NCBI /primer-blast, with a product size <300 bp. SSRs, InDels markers and qPCR primers are listed in Table S2. An InDel marker Indel058 was developed based on the variations in the 5' UTR of *ZmPORB2*.

Plasmid construction and maize transformation

The overexpression vector PZZ0005 was provided by Life Science and Technology Center, China Seed Group Co., Ltd (Wuhan, China). To generate the GRMZM2G073351 over-expression construct, the sequence from ATG-TAG of GRMZM2G073351 was amplified from the maize inbred line B73 by PCR using the gene-specific primers p351-F/R. The PCR product was cloned into PZZ0005 with a homologous recombination clone kit (Vazyme, China). The target gene was driven by the maize Ubiquitin1 (Ubi) promoter. The correct recombinant plasmid was selected by sequencing. The constructs were transformed into the maize inbred line C01 by *Agrobacterium tumefaciens*-mediated transformation (Lin & Zhang, 2005). Primers used are listed in Table S2.

Subcellular localization of *ZmPORB2*

In order to construct the subcellular localization plasmids, the coding sequence without stop codon of *ZmPORB2* was amplified with specific primers ZmPORB-F/R (*Xba*I site) using the cDNA of B73 as the template. The PCR product was inserted into the 35S::GFP (pM999-GFP vector was kindly provided by Shengqian Xia, Huazhong Agricultural University, digested with *Xba*I to construct an ORF encoding a GFP-fused protein driven by the 35S promoter). Maize protoplasts were isolated as described (Yoo *et al.*, 2007) and transformed with the

35S::ZmPORB2-GFP vector using PEG-calcium-mediated method. Transformed protoplasts were cultured at 23°C in the dark overnight. Fluorescence in the transformed protoplasts was imaged using a confocal laser scanning microscope (FV1200, Olympus).

Measurement of tocopherols

The standards for γ-, α-, and δ-tocopherol were purchased from Sigma (St Louis, MO, USA). Total tocopherol content was obtained by summing the three tocopherol forms. The ratio of α- tocopherol to γ- tocopherol was calculated.

Harvested ears were air-dried and shelled, kernels from the middle of ears were dried for 60 hours at 45°C is to eliminate differences in moisture content in different varieties, kept in the dark at 4°C and ground into powder. Samples of leaves and developing kernels/embryos were collected in liquid nitrogen and measured for tocopherol levels in fresh weight. Tocopherol extraction methods refer to previous studies (Chander *et al.*, 2008).

Ultra-performance liquid chromatography (UPLC) from Waters Corporation (Milford, MA, USA) was used for tocopherol measurements using a reverse phase C18 column (BEH, 1.7 μm particle, 2.1 × 100mm). The flow rate was 0.3 mL/min (v/v, 75:25; acetonitrile/methanol containing 0.05% triethylamine and 0.0028% butylated hydroxytoluene). The absorbance of tocopherol was detected at 295 nm using a photo-diode array (PDA) detector. Absorbance, retention time, and phenotypic data were processed with Empower software (Waters Corporation). Three tocopherol (γ-, α-, and δ-) standards, each in eight serial dilutions, were used to construct external standard curves.

RNA extraction, expression analysis and RNA-sequencing data analysis

The collected tissues (leaves and developing kernels) were immediately frozen in liquid nitrogen and stored at -80°C. Total RNA was extracted by using a Quick RNA Isolation kit (Item No: ZH120, HUAYUEYANG, Beijing) according to the user manual. First-strand cDNA was synthesized from total RNA samples using the TransScript One-Step gDNA Removal and cDNA Synthesis SuperMix kit (TransGen, China). Quantitative PCR was performed for gene expression analysis in a BIO-RAD CFX96 Real-Time system using SYBR Green mix (HUAYUEYANG, China) for amplification. The $2^{-\Delta\Delta CT}$ method (Livak & Schmittgen, 2001) was used for relative quantification by using *ZmActin* as an endogenous control. Real-time PCR was performed in three technical replicates. Primers are listed in Table S2.

Total RNA of NP-Leaf, P-Leaf and Kernel samples at 16 DAP of NIL^{K22} and NIL^{CI7} was extracted as described above. High-quality RNA samples were examined by electrophoresis and then used for library construction. Truseq Stranded mRNA sample preparation kit (Low Sample protocol; Illumina, San Diego, USA) was used to construct Illumina stranded mRNA libraries and subjected to pair-end sequencing on Illumina Hiseq 3000 platform. Removal of adapter sequences, poly-N stretches and low-quality reads using Trimmomatic (v3.0) (Bolger *et al.*, 2014). Next, quality of raw sequencing reads in FASTQ format were checked by FASTQC (http://www.bioinformatics.babraham.ac.uk/projects/fastqc/). Tophat2（v2.0.13）(Kim *et al.,* 2013) was used to map the trimmed reads to the maize reference genome B73 (AGPv3). Cufflinks (v2.0.2) (Trapnell *et al.,* 2013) was then used to assemble transcripts and estimate the abundances of genes.

Candidate gene association mapping

Genomic DNA sequences of *ZmPORB2* were obtained by PCR amplification using primers 351F/351R and 5315F/5351R. The PCR products from the AMP508 panel were sequenced. Sequence contig assembly and alignment was performed using BioEdit software. Sites with allelic frequency >0.05 were used for candidate gene association mapping using a mixed linear model (MLM) that accounts for population structure (Q) and kinship (K). Association mapping was implemented in TASSEL3.0 (Bradbury *et al.,* 2007; Yu *et al.,* 2006; Zhang *et al.,* 2010).

Chlorophyll extraction and identification of Chlide a, Pheophorbide a

Collected leaves (100 mg) were flash frozen in liquid nitrogen and grounded. Chlorophyll was extracted and measured according to the previously described method with minor modifications (van Leeuwe *et al.,* 2006). Cold acetone (90% aqueous) was used for extraction (1 mL per 100 mg fresh weight). The extract was subsequently vortexed for 10s, kept in the dark for 30 min at -20 °C, and then transferred on ice in the dark and sonicated for 15min, prior to running through a 0.22 μm filter. The extract was subsequently transferred into a 2 mL ground-glass sample vial and separated using high-performance liquid chromatography (HPLC) as described previously (van Leeuwe *et al.,* 2006). A Thermo Hypersil Gold reverse-phase column (150 × 4.6mm, 5μm; temperature maintained at 28°C) was used and a mobile phase containing (i) acetonitrile:water at 90:10 and (ii) 100% ethyl acetate was adopted. The sample volume for infection was 10 μL, and the flow rate was kept at 0.8 ml /min for 20 min. The gradients used were adapted from Brotas & Plante-Cuny (2003).

Measurement of phytol and Pchlide

Measurement of Pchlide content from leaves was performed using a Plant Protochlorophyllide ELISA Kit following the supplier protocol (LYBD, Beijing).

Phytol was measured using the following supplier protocol (Biotree, Shanghai): Step 1: leaf of moderate amount (100mg±1mg) was placed in a 2ml tube, extracted with 1mL ddH_2O, 0.5 mL ethyl ether, vortexed for 10s. Step 2: the tissue was subsequently homogenized in a commercial ball mill for 4min at 45Hz, and treated ultrasonically for 5min (incubated in ice water) prior to centrifuging for 15 min at 13000 rpm at 4°C to allow for phase separation. Step 3: The organic phase was transferred into a new 1.5 mL tube and added 0.3mL of HPLC-grade water, then repeat step 2 and 3. Step 4: the organic phase was transferred into a new 1.5mL tube, dried through nitrogen flow, then dissolved in 0.2 mL ethyl ether, and finally transferred into a 2 mL glass vial for GC-MS analysis. GC-MS analysis was performed using an Agilent 7890 gas chromatograph system coupled with an Agilent 5975C mass spectrometer. The system utilized a HP-INNOWax capillary column （32m×250μm×0.25μm, J&W Scientific, Folsom, CA, USA). Phytol was silylated and measured by GC-MS as described in Ischebeck *et al*., (2006) and vom Dorp *et al.*, (2015).

Kernel Culture *in vitro*

NIL^{CI7} and NIL^{K22} were grown in the field of Huazhong Agricultural University (Wuhan, Hubei, China). Ears were pollinated at the same stage. Ears at 18 DAP were detached and layers of bract were removed. After sterilized with 75% (v/v) ethanol, the ears were cut into 3-cm thick cob sections. Each cob section retained two or three kernels by peeling off the surrounding kernels. 240 cob sections each genotype were equally divided into two halves. One half was grown in regular culture medium according to Zhang *et al.* (2017), and the other half was grown in culture medium containing 0.1% (v/v) phytol (vom Dorp *et al.*, 2015). Each treatment has 3 repeats with 40 kernels for each repeat. The culture dish were incubated at 25 ± 1°C in darkness for 5 days. The embryos were detached to measure weight and tocopherol content five days after culture.

Accession Numbers

Genes mentioned in this study can be found using the following accession numbers in MaizeGDB: GRMZM2G073351 (*ZmPORB2*) and GRMZM2G036455 (*ZmPORB1*) listed in Figure 3b, GRMZM2G162672 (*CHLG*), GRMZM2G048472 (*VTE2*), GRMZM2G035213 (*VTE4*) and GRMZM2G104538 (*VTE5*) listed in Figure 6.

Sequences of *ZmPORs* and the orthologs from Figure 3a of this study can be found in the EMBL/GenBank database with the following accession numbers: *ZmPORA* (GRMZM2G084958), *ZmPORB1* (GRMZM2G036455), *ZmPORB2* (GRMZM2G073351), *AtPORA* (AT5G54190), *AtPORB* (AT4G27440), *AtPORC* (AT1G03630), *OsPORA* (Os04g58200), *OsPORB* (Os10g35370), *SbPORA* (Sb06g033030) and *SbPORB* (Sb01g018230).

Author contributions

J.Y. and W.Z. designed this study. W.Z., J.L. and Q.P. performed data analysis. S.Y. and Q.K. performed HPLC analyses and metabolite quantifications. W.Z., H.W. and N.N.L. performed UPLC analyses of tocopherol. K.L. performed the transcriptomic analysis. W.L. helped to manage planting, pollination, harvesting of the RIL populations. M.D. performed the subcellular localization of ZmPORB2. W.Z., A.R.F and J.Y. wrote the manuscript.

Acknowledgments

We thank Dr. Bailin Li from DuPont-Pioneer for helping to construct the BAC library of K22 and sequence the target BAC. This research was supported by the National Key Research and Development Program of China (2016YFD0100503, 2016YFD0101003), the National Natural Science Foundation of China (31525017), the Hubei Provincial Natural Science Foundation of China (2015CFA008), and Huazhong Agricultural University Scientific & Technological Self-Innovation Foundation.

Conflict of interest

The authors declare no conflict of interests.

Supporting Information

Figure S1 Confirmation of a major QTL for kernel tocopherol contents on chromosome 5 in three populations in two environments.

Figure S2 Validation of QTL by using progeny test.

Figure S3 Quantification of (a) expression, (b) total tocopherol contents in leaves and (c) total tocopherol contents in kernels in control plants (empty vector; in blue bars) and Zm*PORB2* over-expression lines (*PORB#1, PORB #4* and *PORB#6*; in red bars).

Figure S4 Subcellular localization of ZmPORB2.

Figure S5 Expression patterns of *ZmPORs* in maize inbred B73.

Figure S6 Associations between *ZmPORB2* gene expression (a), total tocopherol content (b) and the 23,582-bp insertion/deletion.

Table S1. *qVE5* information in three linkage populations

Table S2 Primers used in this article.

Data S1 Chlorophyll and Tocopherol-related gene expression in NIL^{K22} and NIL^{CI7} of NP-Leaf, P-Leaf and Kernel at 16 DAP.

References

Azzi, A. (2007). Molecular mechanism of alpha-tocopherol action. *Free Radic. Biol. Med.*, **43**, 16-21.

Beisel, K.G., Jahnke, S., Hofmann, D., Koppchen, S., Schurr, U. and Matsubara, S. (2010). Continuous turnover of carotenes and chlorophyll a in mature leaves of Arabidopsis revealed by $^{14}CO_2$ pulse-chase labeling. *Plant Physiol.*, **152**, 2188-2199.

Bolger, A.M., Lohse, M, and Usadel, B. (2014). Trimmomatic: a flexible trimmer for Illumina sequence data. *Bioinformatics*, **30**, 2114-2120.

Bradbury, P.J., Zhang, Z., Kroon, D.E., Casstevens, T.M., Ramdoss, Y. and Buckler, E.S. (2007). TASSEL: software for association mapping of complex traits in diverse samples. *Bioinformatics*, **23**, 2633-2635.

Brotas, V. and Plante-Cuny, MR. (2003). The use of HPLC pigment analysis to study microphytobenthos communities**.** *Acta Oecologica-Inter J Ecol.*, **24**, S109-S115.

Chander, S., Guo, Y.Q., Yang, X.H., Yan, J.B., Zhang, Y.R., Song, T.M. and Li, J.S. (2008). Genetic dissection of tocopherol content and composition in maize grain using quantitative trait loci analysis and the candidate gene approach. *Mol. Breeding*, **22**, 353-365.

Cheng, Z., Sattler, S., Maeda, H., Sakuragi, Y., Bryant, D.A. and DellaPenna, D. (2003). Highly divergent methyltransferases catalyze a conserved reaction in tocopherol and plastoquinone synthesis in cyanobacteria and photosynthetic eukaryotes. *Plant Cell*, **15**, 2343-2356.

Clarke, M.W., Burnett, J.R. and Croft, K.D. (2008). Vitamin E in human health and disease. *Crit Rev. Clin. Lab. Sci.*, **45**, 417-450.

Collakova, E. and DellaPenna, D. (2003a). The role of homogentisate phytyltransferase and other tocopherol pathway enzymes in the regulation of tocopherol synthesis during abiotic stress. *Plant Physiol.*, **133**, 930-940.

Collakova, E. and DellaPenna, D. (2003b). Homogentisate phytyltransferase activity is limiting for tocopherol biosynthesis in Arabidopsis. *Plant Physiol.*, **131**, 632-642.

DellaPenna, D. (2005). Progress in the dissection and manipulation of vitamin E synthesis. *Trends Plant Sci.*, **10**, 574-579.

DellaPenna, D. and Mène-Saffrané, L. (2011). Vitamin E. *Adv. Bot. Res.*, **59**, 179-227.

Diepenbrock, C.H., Kandianis, C.B., Lipka, A.E. *et al.* (2017). Novel loci underlie natural variation in vitamin E levels in maize grain. *Plant Cell*, **29**, 2374-2392.

Fitzpatrick, T.B., Basset, G.J., Borel, P. *et al.* (2012). Vitamin deficiencies in humans: can plant science help? *Plant Cell*, **24**, 395-414.

Ford, E.S., Schleicher, R.L., Mokdad, A.H., Ajani, U.A. and Liu, S. (2006). Distribution of serum concentrations of alpha-tocopherol and gamma-tocopherol in the US population. *Am. J. Clin. Nutr.*, **84**, 375-383.

Frank, J., Chin, X.W., Schrader, C., Eckert, G.P. and Rimbach, G. (2012). Do tocotrienols have potential as neuroprotective dietary factors? *Ageing Res. Rev.*, **11**, 163-180.

Frick, G., Su, Q., Apel, K. and Armstrong, G.A. (2003). An Arabidopsis porB porC double mutant lacking light-dependent NADPH:protochlorophyllide oxidoreductases B and C is highly chlorophyll-deficient and developmentally arrested. *Plant J.*, **35**, 141-153.

Fu, J, Cheng, Y, Ling, J. *et al.* (2013)**.** RNA sequencing reveals the complex regulatory network in maize kernel. *Nat. Commun.*, **4**, 2832.

Galli, F. and Azzi, A. (2010). Present trends in vitamin E research. *Biofactors*, **36,** 33-42.

Gabruk, M. and Mysliwa-Kurdziel, B. (2015). Light-dependent protochlorophyllide oxidoreductase: phylogeny, regulation, and catalytic properties. *Biochemistry*, **54**, 5255-5262.

Havaux, M., Eymery, F., Porfirova, S., Rey, P. and Dormann, P. (2005). Vitamin E protects against photoinhibition and photooxidative stress in Arabidopsis thaliana. *Plant cell*, **17**, 3451-3469.

Heyes, D.J. and Hunter, C.N. (2005). Making light work of enzyme catalysis: protochlorophyllide oxidoreductase. *Trends Biochem. Sci.*, **30**, 642-649.

Hörtensteiner, S. (2013). Update on the biochemistry of chlorophyll breakdown. *Plant Mol. Biol.*, **82**, 505-517.

Hörtensteiner, S. and Kräutler, B. (2011). Chlorophyll breakdown in higher plants. *Biochim. Biophys. Acta.*, **1807**, 977-988.

Horvath, G., Wessjohann, L., Bigirimana, J., Jansen, M., Guisez, Y., Caubergs, R. and Horemans, N. (2006). Differential distribution of tocopherols and tocotrienols in photosynthetic and non-photosynthetic tissues. *Phytochemistry*, **67**, 1185-1195.

Ischebeck, T., Zbierzak, A.M., Kanwischer, M. and Dormann, P. (2006). A salvage pathway for phytol metabolism in Arabidopsis. *J. Biol. Chem.*, **281**, 2470-2477.

Jiang, T., Christian, P., Khatry, S.K., Wu, L. and West, K.P. (2005). Micronutrient deficiencies in early pregnancy are common, concurrent, and vary by season among rural Nepali pregnant women. *J. Nutr.*, **135**, 1106-1112.

Kim, D., Pertea, G., Trapnell, C., Pimentel, H., Kelley, R. and Salzberg, S.L. (2013). TopHat2: accurate alignment of transcriptomes in the presence of insertions, deletions and gene fusions. *Genome Biol.*, **14**, R36.

Ledford, H.K., Baroli, I., Shin, J.W., Fischer, B.B., Eggen, R.I. and Niyogi, K.K. (2004). Comparative profiling of lipid-soluble antioxidants and transcripts reveals two phases of photo-oxidative stress in a xanthophyll-deficient mutant of Chlamydomonas reinhardtii. *Mol. Genet. Genomics.*, **272**, 470-479.

Li, Q., Yang X., Xu, S., Cai, Y., Zhang, D., Han, Y., Li, L. *et al*. (2012). Genome-wide association studies identified three independent polymorphisms associated with alpha-tocopherol content in maize kernels. *PloS ONE*, **7**, e36807.

Lipka, A.E., Gore, M.A., Magallanes-Lundback, M. *et al*. (2013). Genome-wide association study and pathway-level analysis of tocochromanol levels in maize grain. *G3*., **3**, 1287–1299.

Lin, Y.J. and Zhang, Q. (2005). Optimising the tissue culture conditions for high efficiency transformation of indica rice. *Plant Cell Rep.*, **23**, 540-547.

Lin, Y.P., Wu, M.C. and Charng, Y.Y. (2016). Identification of a chlorophyll dephytylase involved in chlorophyll turnover in Arabidopsis. *Plant Cell*, **28**, 2974-2990.

Lin, Y.P., Lee, T.Y., Tanaka, A. and Charng, Y.Y. (2014). Analysis of an Arabidopsis heat-sensitive mutant reveals that chlorophyll synthase is involved in reutilization of chlorophyllide during chlorophyll turnover. *Plant J.*, **80**, 14-26.

Liu, H., Wang, F., Xiao, Y. *et al*. (2016). MODEM: multi-omics data envelopment and mining in maize. *Database (Oxford)*, **2016**, 1-9.

Livak, K.J. and Schmittgen, T.D. (2001). Analysis of relative gene expression data using real-time quantitative PCR and the $2^{-\Delta\Delta CT}$ method. *Methods*, **25**, 402–408.

Maeda, H. and DellaPenna, D. (2007). Tocopherol functions in photosynthetic organisms. *Curr. Opin. Plant Biol.*, **10**, 260-265.

Masuda, T., Fusada, N., Oosawa, N. *et al.* (2003). Functional analysis of isoforms of NADPH: protochlorophyllide oxidoreductase (POR), PORB and PORC, in Arabidopsis thaliana. *Plant Cell Physiol.*, **44**, 963-974.

Matile, P., Hörtensteiner, S. and Thomas, H. (1999). Chlorophyll degradation. *Annu. Rev. Plant Physiol. Plant Mol. Biol.*, **50**, 67-95.

Mene-Saffrane, L. and DellaPenna, D. (2010). Biosynthesis, regulation and functions of tocochromanols in plants. *Plant Physiol. Biochem.*, **48**, 301-309.

Pan, Q., Li, L., Yang, X. *et al.* (2016). Genome-wide recombination dynamics are associated with phenotypic variation in maize. *New Phytol.*, **210**, 1083-1094.

Péter, S., Friedel, A., Roos, F.F., Wyss, A., Eggersdorfer, M., Hoffmann, K., Weber, P. (2016)**.** A systematic review of global alpha-tocopherol status as assessed by nutritional intake levels and blood serum concentrations. *Int. J. Vitam. Nutr. Res.*, **14**, 1–21.

Pokorska, B., Zienkiewicz, M., Powikrowska, M., Drozak, A. and Romanowska, E. (2009). Differential turnover of the photosystem II reaction centre D1 protein in mesophyll and bundle sheath chloroplasts of maize. *Biochim. Biophys. Acta.*, **1787**, 1161-1169.

Reinbothe, S., Reinbothe, C., Holtorf, H. and Apel, K. (1995). Two NADPH: protochlorophyllide oxidoreductases in barley: evidence for the selective disappearance of pora during the light-induced greening of etiolated seedlings. *Plant Cell*, **7**, 1933-1940.

Sakuraba, Y., Rahman, M.L., Cho, S.H., Kim, Y.S., Koh, H.J., Yoo, S.C., and Paek, N.C. (2013). The rice faded green leaf locus encodes protochlorophyllide oxidoreductase B and is essential for chlorophyll synthesis under high light conditions. *Plant J.*, **74**, 122-133.

Sattler, S.E., Gilliland, L.U., Magallanes-Lundback, M., Pollard, M. and DellaPenna, D. (2004). Vitamin E is essential for seed longevity and for preventing lipid peroxidation during germination. *Plant Cell*, **16**, 1419-1432.

Schelbert, S., Aubry, S., Burla, B., Agne, B., Kessler, F., Krupinska, K. and Hörtensteiner, S. (2009). Pheophytin pheophorbide hydrolase (pheophytinase) is involved in chlorophyll breakdown during leaf senescence in Arabidopsis. *Plant Cell*, **21**, 767-785.

Scrutton, N.S., Groot, M.L. and Heyes, D.J. (2012). Excited state dynamics and catalytic mechanism of the light-driven enzyme protochlorophyllide oxidoreductase. *Phys. Chem. Chem. Phys.*, **14**, 8818-8824.

Shintani, D. and DellaPenna, D. (1998). Elevating the vitamin E content of plants through metabolic engineering. *Science*, **282,** 2098-2100.

Trapnell, C., Hendrickson, D.G., Sauvageau, M., Goff, L., Rinn, J.L. and Pachter, L. (2013). Differential analysis of gene regulation at transcript resolution with RNA-seq. *Nat. Biotechnol.*, **31**, 46-53.

Tyystjärvi, E. (2013). Photoinhibition of Photosystem II. *Int. Rev. Cell Mol. Biol.*, **300**, 243-303.

Valentin, H.E., Lincoln, K., Moshiri, F. *at al.* (2006). The Arabidopsis vitamin E pathway gene5-1 mutant reveals a critical role for phytol kinase in seed tocopherol biosynthesis. *Plant Cell*, **18**, 212-224.

Van Eenennaam A.L., Lincoln K., Durrett T.P. *et al*. (2003). Engineering vitamin E content: from *Arabidopsis* mutant to soy oil. *Plant Cell*, **15**, 3007-3019.

Van Leeuwe, M.A., Villerius, L.A., Roggeveld, J., Visser, R.J.W., and Stefels, J. (2006). An optimized method for automated analysis of algal pigments by HPLC. *Mar. Chem.*, **102**, 267-275.

Vavilin, D. and Vermaas, W. (2007). Continuous chlorophyll degradation accompanied by chlorophyllide and phytol reutilization for chlorophyll synthesis in *Synechocystis* sp. PCC 6803. *Biochim. Biophys. Acta.*, **1767**, 920-929.

Vom Dorp, K., Holzl, G., Plohmann, C.*et al.* (2015). Remobilization of phytol from chlorophyll degradation is essential for tocopherol synthesis and growth of Arabidopsis. *Plant Cell*, **27**, 2846-2859.

Wang, S., Basten, C.J. and Zeng, Z.B. (2012). Windows QTL cartographer version 2.5.Raleigh, North Carolina: Statistical genetics, North Carolina State University.

Wang, H., Xu, S., Fan, Y. *et al*. (2018). Beyond pathways: genetic dissection of tocopherol content in maize kernels by combining linkage and association analyses. *Plant Biotechnol J.*, doi: 10.1111/pbi.12889.

Wolf, G. (2005). The discovery of the antioxidant function of vitamin E: the contribution of Henry A. *Mattill. J. Nutr.*, **135**, 363-366.

Wong, J.C., Lambert, R.J., Wurtzel, E.T. and Rocheford, T.R. (2004). QTL and candidate genes phytoene synthase and zeta-carotene desaturase associated with the accumulation of carotenoids in maize. *Theor. Appl. Genet.*, **108**, 349-359.

Xiao, Y., Tong, H., Yang, X. *et al*. (2016). Genome-wide dissection of the maize ear genetic architecture using multiple populations. *New Phytol.*, **210,** 1095-1106.

Xiao, Y., Liu, H., Wu, L., Warburton, M., and Yan, J. (2017) Genome-wide association studies in maize: praise and stargaze. *Mol. Plant.*, **10**, 359-374.

Xu, S., Zhang, D., Cai, Y.*et al.* (2012). Dissecting tocopherols content in maize (Zea *mays* L.), using two segregating populations and high-density single nucleotide polymorphism markers. *BMC Plant Biol.*, **12**, 201.

Yang, X., Gao, S., Xu, S.*et al.* (2011). Characterization of a global germplasm collection and its potential utilization for analysis of complex quantitative traits in maize. *Mol. Breeding*, **28**, 511-526.

Yoo, S.D., Cho, Y.H. and Sheen, J. (2007). Arabidopsis mesophyll protoplasts: A versatile cell system for transient gene expression analysis. *Nat. Protoc.*, **2**, 1565–1572.

Yu, J., Pressoir, G., Briggs, W.H., Vroh B.I. *et al*. (2006). A unified mixed-model method for association mapping that accounts for multiple levels of relatedness. *Nat. Genet.*, **38**, 203-208.

Zeng, Z.B., Kao, C.H. and Basten, C.J. (1999). Estimating the genetic architecture of quantitative traits. *Genet. Res.*, **74**, 279-289.

Zhang, C., Zhang, W., Ren, G. *et al.* (2015). Chlorophyll synthase under epigenetic surveillance is critical for vitamin e synthesis, and altered expression affects tocopherol levels in Arabidopsis. *Plant Physiol.*, **168**, 1503-1511.

Zhang, L., Li, X.H., Gao, Z., Shen, S., Liang, X.G., Zhao, X., Lin, S., and Zhou, S.L. (2017). Regulation of maize kernel weight and carbohydrate metabolism by abscisic acid applied at the early and middle post-pollination stages in vitro. *J Plant Physiol*., **216**, 1-10.

Zhang, W., Liu, T., Ren, G., Hörtensteiner, S., Zhou, Y., Cahoon, E.B., and Zhang, C. (2014). Chlorophyll degradation: the tocopherol biosynthesis related phytol hydrolase in Arabidopsis seeds is still missing. *Plant Physiol.*, **166**, 70-79.

Zhang, Z., Ersoz, E., Lai, C.Q. *et al*. (2010). Mixed linear model approach adapted for genome-wide association studies. *Nat. Genet*., **42**, 355-360.

Figure 1. Schematic view of chlorophyll metabolism in producting free phytol involved in tocopherol biosynthetic pathways (modified from Chander *et al* 2008 and Hörtensteiners 2013).

The phytol moiety of tocopherols could be derived from chlorophyll turnover (purple arrows) and chlorophyll breakdown (sky-blue arrows), respectively. The enzymes in red have been identified as key genes for tocopherol synthesis and chlorophyll metabolism in previous studies; Abbreviations for enzymes and compounds in this pathway are as follows: CHLG, chlorophyll synthase; CLD1, chlorophyll dephytylase1; CLH, chlorophyllase; GGR, geranylgeranyl reductase; NCCs, nonfluorescent chlorophyll catabolites; PAO, pheophorbide a oxygenase; Phytyl-P, phytyl phosphate; Phytyl-PP, phytyl diphosphate; PORB, protochlorophyllide oxidoreductase B; PPH, pheophytin hydrolase; SGR, STAY-GREEN (chlorophyll a Mg-dechelatase).

Figure 2. Map-based cloning of *qVE5*.

(a) Location of *qVE5* on chromosome 5, mapped in K22/CI7 F_6 population in 2011 in two environments. (b) Bin map of HIF1171-2 with a heterozygous region on chromosome 5 indicated by cross-hatching. (c) Genotypes and phenotypes of the HIF-1171-2 (K22 and CI7) and eight homozygous segmental isogenic lines developed from 2013 and 2014 carrying crossovers around *qVE5*. Two asterisks indicate significant differences in tocopherol content against HIF1171-2 (K22 haplotype) at the $P < 0.01$ level and no asterisks means no significant difference at the $P < 0.05$ level. (d) The blue square shows the target gene. Information of GRMZM2G073351 is according to B73 AGPv2 genome. Red triangle shows K22 unique sequence against B73 genome. Blue vertical shows B73 unique sequence against K22. Trait abbreviations: γ, γ-tocopherol content; α, α-tocopherol content; T, total tocopherol content; Values are shown in means ± S.D.; unit: μg/g. n, number of evaluated individuals in each homozygous segmental isogenic line.

Figure 3. Phylogenetic tree of PORs in plants and the effect of light on *ZmPORBs* expression.

(a) Protein sequences of PORs from maize, *Arabidopsis*, *Oryza sativa*, sorghum are obtained from GenBank. The phylogenetic analysis was conducted with MEGA 7.0 using the neighbor-joining method. In the x-dimension, branch length represents evolutionary distance (number of amino acid differences per site). Bootstrap values were calculated from 1000 replicates. (b) B73 lines at five-leaf stage were grown under short day (SD) and long day (LD) conditions (cool white light, 500 μmol m^{-2} s^{-1}) in the greenhouse. The mean of each point is based on the average of three biological repeats calculated using the relative quantification method. The black bars indicate the dark period, and the white bars indicate the light period. The numbers below the bars indicate hours from start of sampling. Error bars, S.D.

Figure 4. Causal sites identification and functional analysis of *ZmPORB2*.

(a) Association between tocopherol content and the polymorphisms of *ZmPORB2* in a panel of 508 lines. Physical locations of the markers are shown in the x-axis, and the –log base 10 P-values from the mixed linear model are shown in the y-axis. Indel058 are highlighted in red and blue. (b) The gene structure of *ZmPORB2* (exons, black boxes; untranslated regions, open boxes). (c) LD analysis. Pairwise R^2 value between all polymorphic sites in *ZmPORB2* are shown, where the color of each box corresponds to the R^2 value according to the legend.(d) Haplotypes of Indel058 among maize the parents of RIL populations.(e) Tocopherol content from the AMP508 panel grouped by with/without the 0/5/8 insertion in 5'UTR of *ZmPORB2*. For (e), the maximum, 75% quartile, median, 25% quartile, and minimum expression levels are shown. The P-values are based on Student's t-tests. Population abbreviations: BB, B73/BY804; KC, K22/CI7; ZY, ZONG3/YU8701

Figure 5. *ZmPORB2* expression and leaf tocopherol content after pollination.

(a) Relative expression levels of *ZmPORB2* in kernels, NP-Leaf and P-leaf after pollination. (b) γ-, α-, total tocopherol content in NP-leaf. (c) γ-, α-, total tocopherol content in P-leaf. P, pollinated; NP, non-pollinated. Tocopherol contents and expression levels are shown in means ± S.D. Unit: μg/g; n=10; Student's *t*-test; error bars, S.D. Two asterisks, $P < 0.01$; one asterisk, $P < 0.05$; no asterisks, $P > 0.05$. Tocopherol content in leaves is in fresh weight.

NIL^{CI7} and NIL^{K22} are near isogenic lines produced in the positional cloning process, which share the same genetic background and differ only in the *ZmPORB2* genomic region with the parents' genotypes.

Figure 6. Quantification of metabolites and gene expression associated with tocopherol biosynthesis pathway in leaves.

Content of (a) Chlorophyll a+b between P-Leaf and NP-Leaf at different time points; Content of (b) Protochlorophyllide, (c) Chlorophyllide a, (d) Pheophorbide a, (e) Phytol between P-Leaf and NP-Leaf at 12 DAP. Expression levels of (f) *CHLG* (Chlorophyll synthase) in P-Leaf and NP-Leaf. Expression levels of (g) *VTE2* (homogentisate phytyltransferase), (h) *VTE4* (γ-tocopherol methyltransferase), (i) *VTE5* (phytol kinase) in P-Leaf. P, pollinated; NP, non-pollinated. Metabolites contents and expression levels are shown in means ± S.D.; n=10; Student's t-test; error bars, S.D. Metabolites in leaves is in fresh weight. Two asterisks, $P < 0.01$; one asterisk, $P < 0.05$; no asterisks, $P > 0.05$.

Figure 7. Reciprocal crosses of *ZmPORB2* NILs show tocopherol determined by genotype of leaves.

γ-, α-, total tocopherol content in in mature kernels of selfed and cross-pollinated NILs. Tocopherol contents and expression levels are shown in means ± S.D. Unit: μg/g; n=14; Student's t-test; error bars, S.D. Two asterisks, $P < 0.01$; no asterisks, $P > 0.05$. NIL^{CI7K22} referring to the kernels from NIL^{CI7} plant pollinated with NIL^{K22} pollen, NIL^{K22CI7} referring to the kernels from NIL^{K22} plant pollinated with NIL^{CI7} pollen.

Figure 8. *In vitro* cultured maize kernels.

(a) embryo fresh weight, (b) total tocopherol content in embryo (in fresh weight) and (c) *ZmPORB2* expression levels of embryo at 18 DAP and 23 DAP in plants, *in vitro* cultured kernels of 18 DAP without phytol and with phytol for five days. Phenotypic data and expression levels are shown in means ± S.D.; n=3; bars superscripted by different lowercases show significant differences at 0.01 probability level; Data were analyzed using one-way analysis of variance (ANOVA) and Tukey's test.

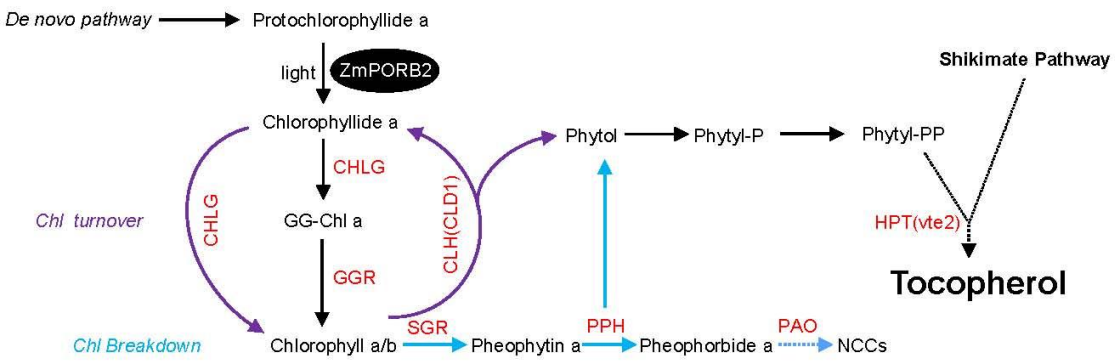

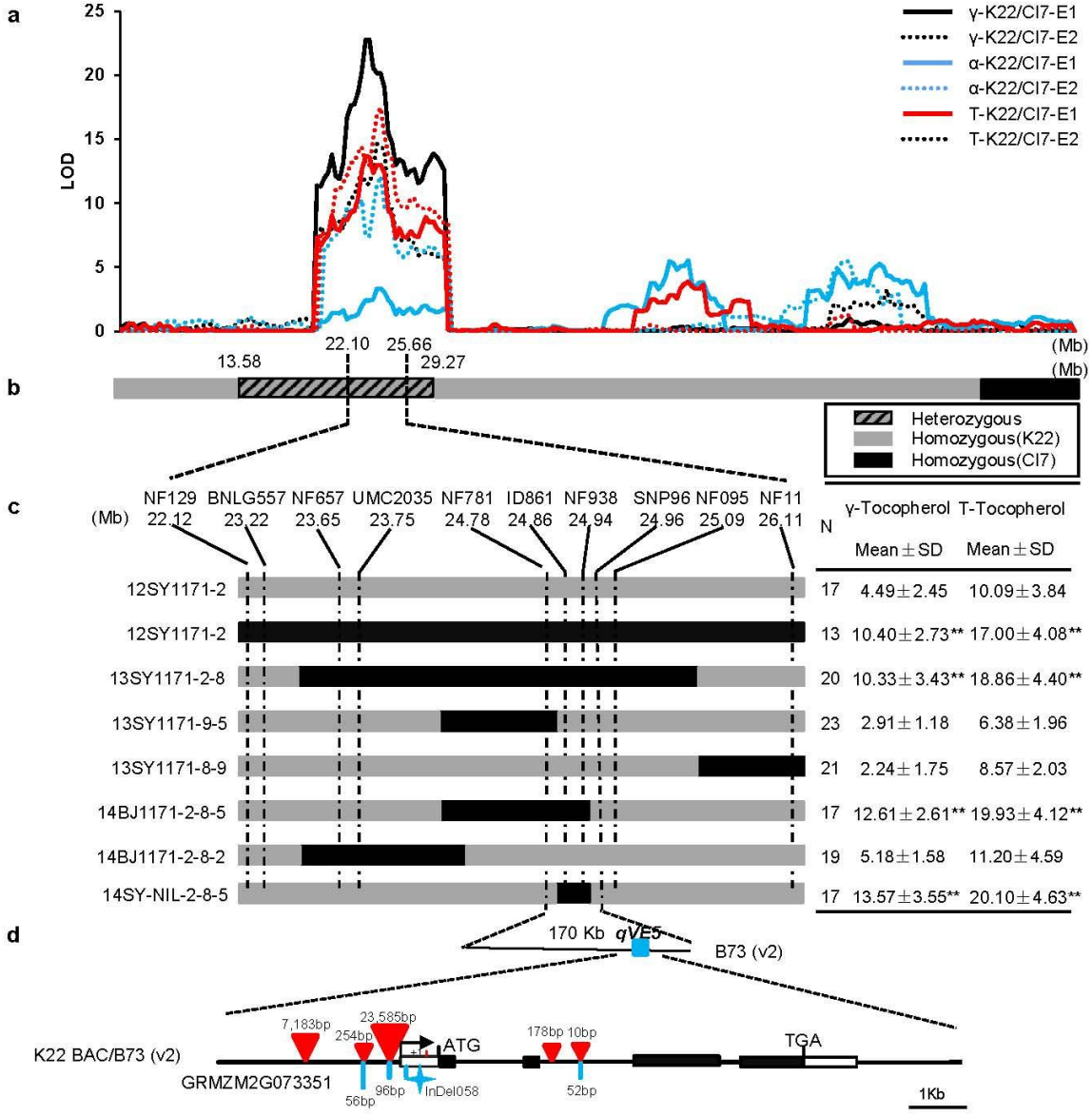

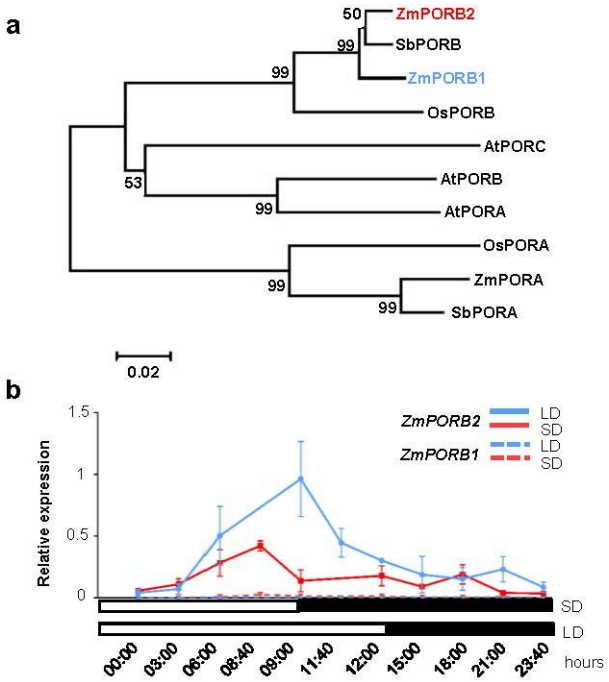

a

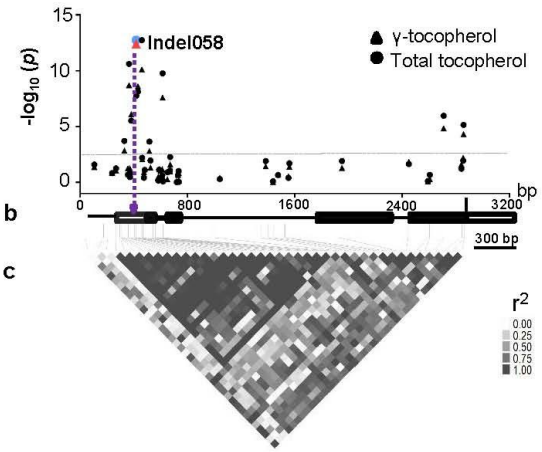

b

c

e

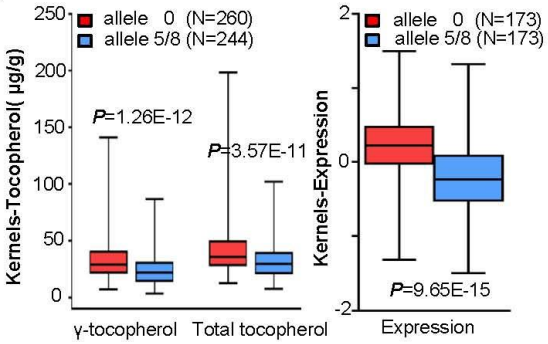

d

Populations	Parents	Total tocopherol(mean±SD)	Value	InDel058	Numbers in AMP
BB	BY804	156.22±1.52μg	Higher	allele 0	allele 0(260)
	B73	34.07±3.04μg	Lower	allele 5	
KC	CI7	11.09±1.96μg	Higher	allele 0	allele 5(76)
	K22	22.99±2.09μg	Lower	allele 8	
ZY	ZONG3	26.14±0.73μg	Higher	allele 0	allele 8(168)
	YU8701	22.89±1.08μg	Lower	allele 8